

# ONLINE-MONITORING OF CARBON FIBER REINFORCED PLASTICS USING SILVER NANOPARTICLE BASED INK

Till Augustin<sup>1</sup>, Hauke H. Langner<sup>2</sup>, Vico Haverkamp<sup>2</sup>, and Bodo Fiedler<sup>1</sup>

<sup>1</sup>Institute of Polymer Composites, Technische Universität Hamburg,  
Denickestraße 15, 21073 Hamburg, Germany

Email: [till.augustin@tuhh.de](mailto:till.augustin@tuhh.de), Web Page: <http://www.tuhh.de/kvweb>

Email: [fieder@tuhh.de](mailto:fieder@tuhh.de), Web Page: <http://www.tuhh.de/kvweb>

<sup>2</sup>Institute of Automation Technology, Helmut-Schmidt-Universität,  
Holstenhofweg 85, 22043 Hamburg, Germany

Email: [langnerh@hsu-hh.de](mailto:langnerh@hsu-hh.de), Web Page: <http://www.hsu-hh.de/pdv/>

Email: [haverkav@hsu-hh.de](mailto:haverkav@hsu-hh.de), Web Page: <http://www.hsu-hh.de/pdv/>

**Keywords:** Structural health-monitoring, CFRP, ink-jet printing, conductive paths, surface cracks

## Abstract

In this study, we present an online-monitoring approach using silver nanoparticle based ink on carbon fiber reinforced plastics (CFRP). After production of CFRP plates in a prepreg autoclave process and printing conducting paths on the material, we investigate the interface of CFRP and conducting paths of printed silver nanoparticle based ink by light microscopy. Mechanical tests with simultaneous electrical resistance measurement demonstrate the applicability of the presented method for a structural health-monitoring system. Delaminations can be detected and localized inside of the material by electrical through thickness measurements. Furthermore, resistance measurements of the conductive paths allow for surface crack detection and might be established as alternative method to other structural health-monitoring methods.

## 1. Introduction

Carbon fiber reinforced plastics (CFRP) are widely used in various industries such as aircraft, aerospace, automotive, and wind energy. To assure integrity and avoid catastrophic structural failures, usually periodic inspections are carried out, which can be time-consuming and costly especially for large structures due to expensive non-destructive testing (NDT) processes and downtime. Hence, a permanent monitoring of the integrity of the structure during operation, namely a structural health-monitoring (SHM) system, is valuable in many cases. SHM offers a high potential to increase safety, reliability, and cost efficiency of fiber reinforced structures.

Several approaches for monitoring composite structures exist [1–6]. One promising SHM method for materials which are not electrically insulating is the electrical resistance measurement [7]. In CFRP, the carbon fibers are electrically conductive and the polymer matrix is non-conductive. The high electrical conductivity of carbon fibers allows for *in situ* strain monitoring and damage detection by electrical resistance measurements [8–13].

To exploit the electrical conductivity of CFRP and use the material itself as a sensor in an SHM system a reliable contacting of the material is crucial to enable electrical resistance measurement during operation. Due to its excellent reproducibility and high potential for industrial automation, ink-jet printing is a promising technology to place conducting paths on the material and realize reliable contacts for electrical resistivity measurements [14–17].

## 2. Materials and specimen preparation

### 2.1. CFRP specimens

The used carbon fiber reinforced prepregs consist of an epoxy matrix and carbon fibers (Hexply M21/34%/UD194/T800S by Hexcel) and have a fiber volume content of  $57.77 \pm 0.01$  % (measured on 8 samples of the cured carbon fiber laminates according to DIN EN 2564). CFRP plates with the laminate layup  $[90_3 / 0_2]_s$  were laminated from the prepregs and cured in an autoclave process at a temperature of 180 °C and a pressure of 7 bar for 120 minutes in a nitrogen atmosphere. Subsequently, specimens with dimensions of 100 mm x 15 mm x 1.875 mm (in accordance with DIN EN ISO 14125) were cut from the plates using a water-lubricated diamond saw.

### 2.2 Printed conductive paths

Functional silver-ink was printed on the CFRP surface to obtain conductive paths. Silver nanoparticles (31.0 wt.-%) with a D90 value (90 percent of the distribution lies below this value) of 60 nm were dispersed in the solvent butyl carbitol (68.5 wt.-%). The density of the ink is 1.48 g/ml and the viscosity measures 17.6 mPas at a shear rate of  $1000 \text{ s}^{-1}$  at room temperature. For steric stabilization, 0.5 wt.-% ethyl cellulose was added which assures a stable suspension for about three hours. Thus, during the printing process the composition of the ink is constant. The used single nozzle print head (by microdrop Technologies) has a nozzle diameter of 70  $\mu\text{m}$ . A piezo actor controls the emission of single drops. The voltage and the current pulse applied to the piezo actor as well as the nozzle temperature can be varied to obtain an optimal drop. The control software and the moveable table where the substrate is placed on allow for printing images on the CFRP. This system forms a reliable and reproducible drop with the ink as described above. The smaller the size of the silver particles, the higher the corresponding surface-volume ratio, which is accompanied with the surface energy. Therefore, in the sintering process the thermal energy can be reduced. Here, a temperature of 170 °C was applied for four hours to obtain conductive silver paths.

### 2.3. Specimen preparation

To enable reliable contacting with the system for resistance measurements stranded copper wires were connected with the printed conductive paths using conductive silver paint. After finished preparation, the specimens were dried for five hours at 40°C in a vacuum oven and stored in a desiccator until testing to keep the specimen conditions constant.

## 3. Experimental

### 3.1. Test setup

We conducted three-point bending tests using a universal testing machine (Zwick Z2.5 TH). The test speed was set to 2 mm/min to generate a sufficient time interval between the individual failures to detect the failures separately. Ceramic cylinders ( $\text{Al}_2\text{O}_3$ ) ensure electric insulation of the specimens during testing. The distance between the lower cylinders is 55 mm and the diameters are 10 mm and 4 mm for the upper and lower cylinders, respectively.

Two different test series were conducted described in the following. In the first test setup conductive paths are printed parallel to the 100 mm long edges and the resistance is measured along these paths to investigate the change of resistance along the paths exposed to bending. In addition, tests with printed paths on both sides of the specimens are tested and the resistance is measured through the material during mechanical testing.

### 3.2. Electrical resistance measurements along printed paths

The specimen geometry and the locations of the conductive paths are shown in Figure 1 (a). Two paths are printed on the bottom side of the specimen. The number of two paths enables to compare two measured signals of paths lying next to each other. To measure the DC resistance over the length of the conductive paths the ends of the paths are connected with a digital multimeter (Keithley 2000). Figure 1 (b) shows a schematic of the test setup.

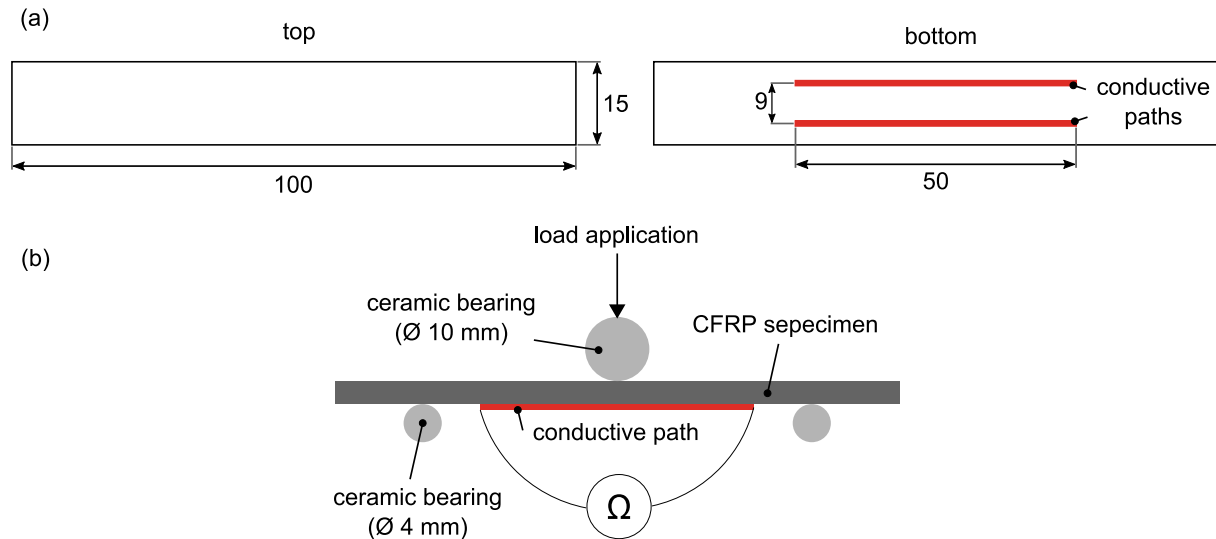


**Figure 1.** (a) Specimen geometry, design of conductive paths for measuring resistance along printed paths, (b) Three-point bending test setup with electrical resistance measurement along printed paths

### 3.3. Electrical measurement through material

To be able to measure the resistance through the material, specimens with printed paths on both sides are produced. The design of the conductive paths for measuring through the material is shown in Figure 2 (a). The DC resistance is measured from the top electrode to each of the four electrodes on the bottom side of the specimen. Figure 2 (b) shows the test setup and the connected electrodes for the four measured resistances.

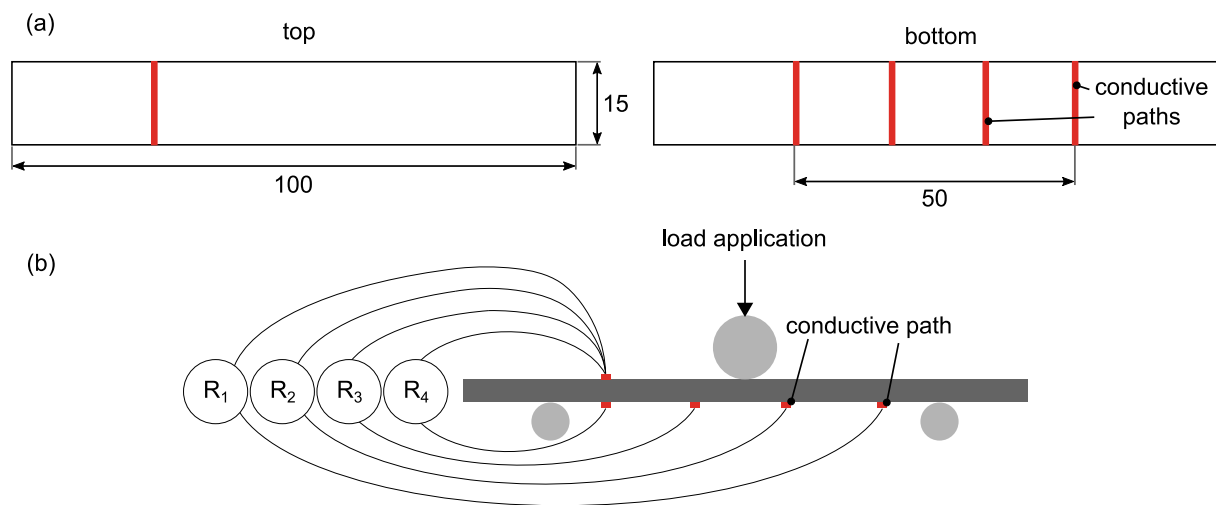


**Figure 2.** (a) Specimen geometry, design of conductive paths for measuring resistance through material, (b) Three-point bending test setup with four-channel electrical resistance measurement through material

## 4. Results

### 4.1. Electrical resistance measurement along printed paths

Figure 3 shows the results of the mechanical and electrical measurements for a specimen with typical characteristics. The resistance without loading ( $R_0$ ) is  $2.1 \Omega$  for both conductive paths, and the resistance change ( $\Delta R$ ) is specified as the difference of the measured resistance without ( $R_0$ ) and during loading ( $R$ ).

The force increases to a maximum at a displacement of 14.8 mm and fracture of the specimen occurs at 18.7 mm. In addition to the mechanical response, the change of electrical resistance is shown for the two conductive paths, measured from one end to the other of the same path, respectively. Both, the force-displacement curve and the resistance change-displacement curves contain several discontinuities indicated by circles in the diagram. The discontinuities correlate perfectly with the steps in the resistance change.

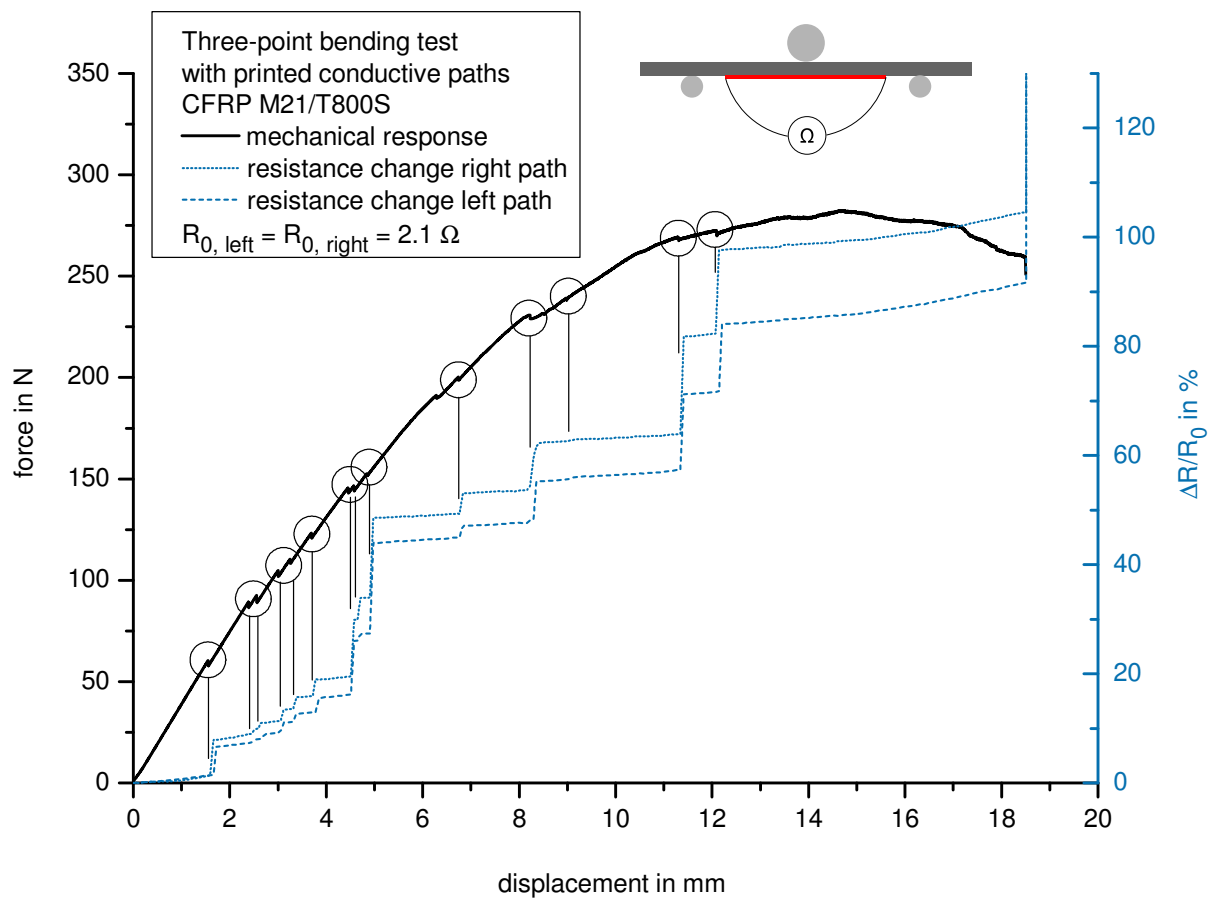


**Figure 3.** Force and resistance change of conductive paths versus displacement

The discontinuities in the measured force are present due to damages in the material. Since the dominating failure modes in cross-ply laminates subjected to bending and the failures observed in the tested specimens are inter-fiber failure and delamination, these two failure modes correspond to the discontinuities of the measured force and resistance signals. All failures detected by the measured force and therefore all inter-fiber failures and delaminations exceeding a certain amount of energy release can be detected by resistance changes. The resistance increase at the end of the test (up to unmeasurable values) indicates the final fracture of the specimen cutting the specimen completely and therefore all possible conductive paths for current flow. Hence, all failures exceeding a certain size and

therefore being relevant for the integrity of the specimen as well as the final fracture can be detected reliably.

Light microscopy observations of the damaged printed paths show that inter-fiber failures at the surface cause interruptions as well as flaking of the paths in proximity to the cracks (see Figure 4). Hence, when inter-fiber failures occur the resistance increases due to the interruption of the paths in the region of the cracks at the surface. The current flow in case of inter-fiber failures flows through the CFRP, which has a higher resistance compared to the silver based printed path resulting in a resistance increase. The current flow is schematically shown in Figure 5.

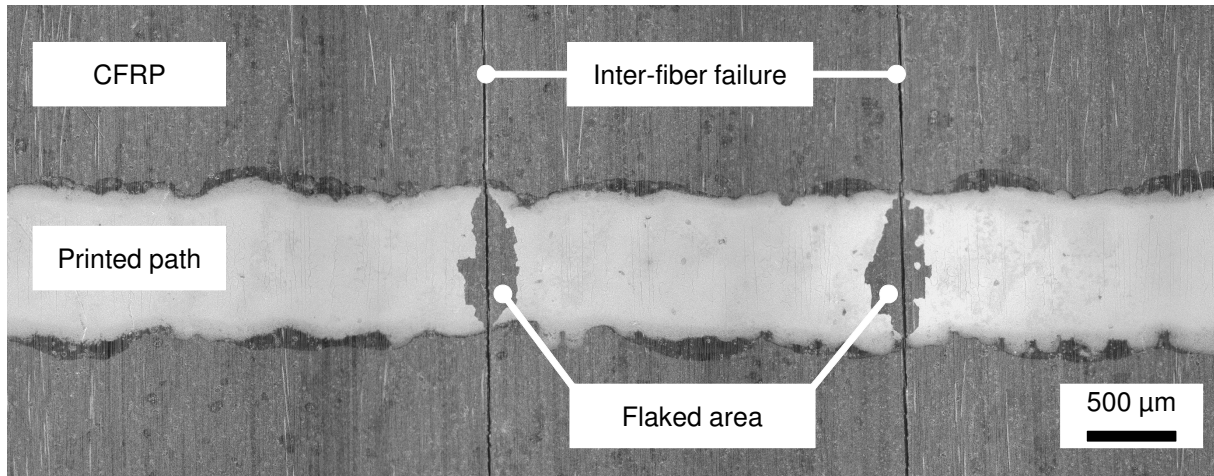


**Figure 4.** Light microscopy observation of printed path after testing

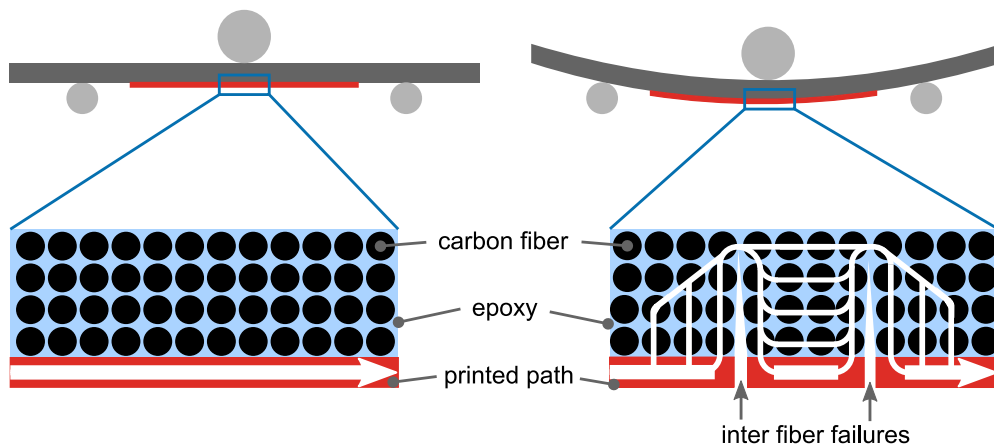


**Figure 5.** Schematic of current flow (white arrows); left: through undamaged printed path; right: through damaged printed path and composite material in case of inter fiber failures

This method enables to detect inter-fiber failures reliably on the surface. It can be used to monitor surfaces where surface cracks are crucial.

#### 4.2. Electrical measurement through material

Mechanical and electrical measurements for a typical behaving specimen are plotted in Figure 6. The mechanical response is qualitatively the same as in Figure 3. The resistance changes are different for the four measured channels. For channel 1 (from top electrode to low electrode 1) and channel 4 (from top electrode to low electrode 4) the relative resistance change is in the range of  $\pm 2.5\%$  until final fracture where the resistances suddenly increase to infinity. The resistance change of channels 2 and 3

(from top electrode to lower middle electrodes) increases significantly with increasing displacement up to 26 % and 17.5 % before final failure, respectively.

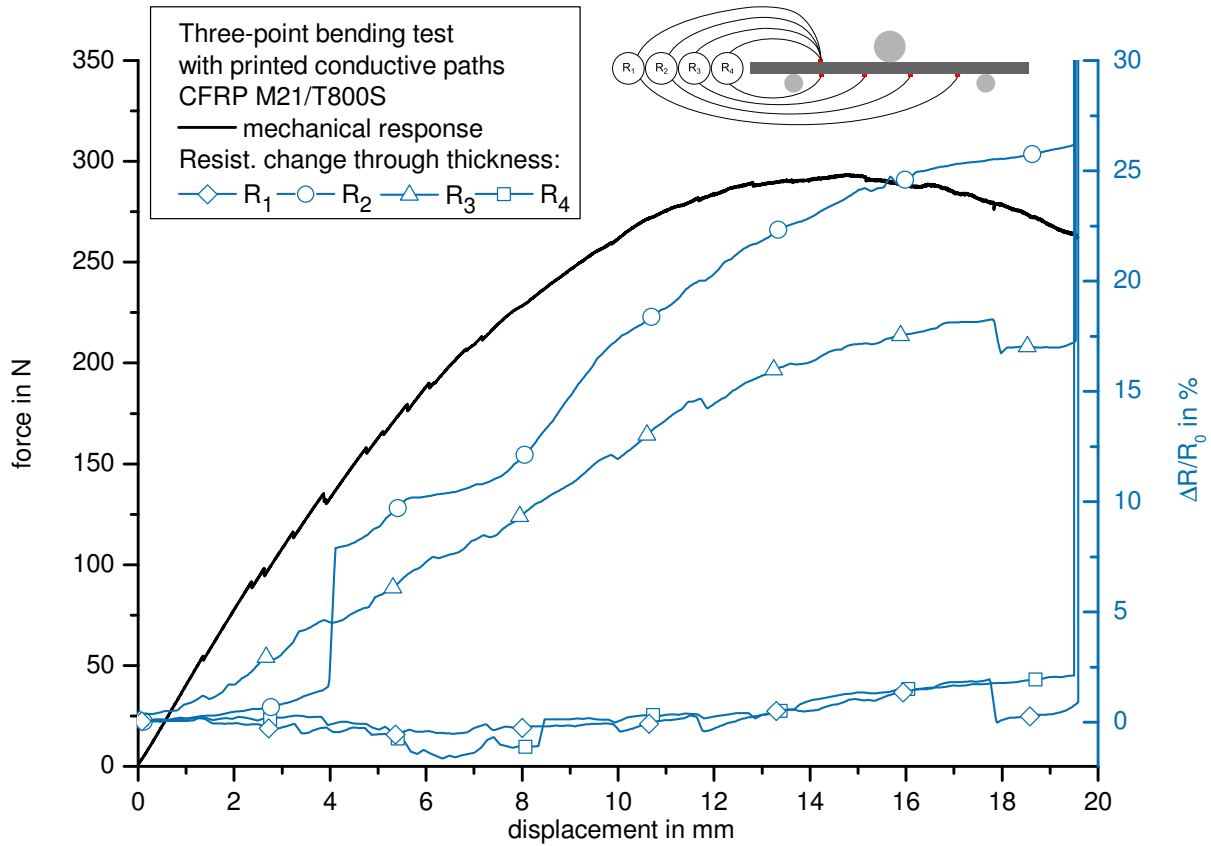


**Figure 6.** Force and resistance change of the four measured channels versus displacement

The non-significant resistance changes of channel 1 and 4 (to electrodes left end right of the specimens) indicate that the current flow is not changed significantly. It is assumed that close to these electrodes no delaminations and inter-fiber failures that interrupt the current flow are present. For channel 2 and 3 the resistance increase indicates that damages occur inside of the material close to the most stressed areas in the center of the specimen. This can be proven by light microscopy observations of a tested specimen shown in Figure 7. Above electrodes 2 and 3 (center electrodes), inter-fiber failures in the three lower 90°-layers and delaminations in between the 0° and 90°-layer are found. Above the outer electrodes (1 and 4) only inter-fiber failures are detected by light microscopy.

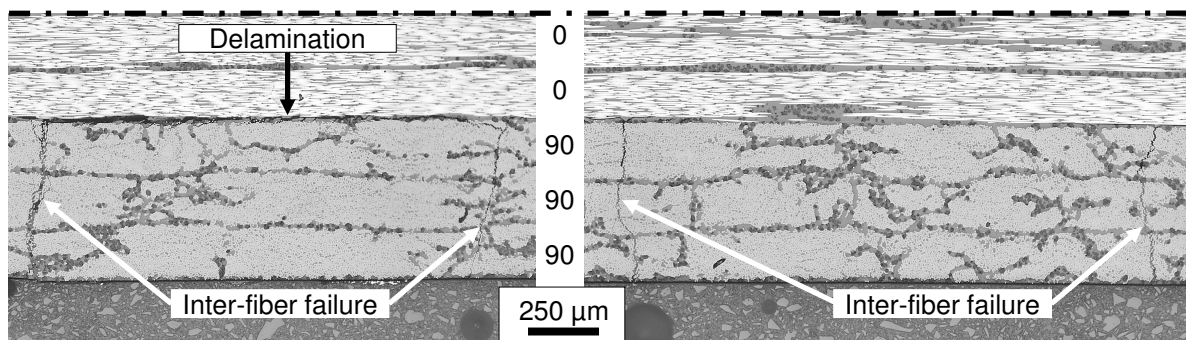


**Figure 7.** Light microscopy observation after testing of polished sections. Left: Region above electrodes 2 and 3 (middle electrodes), inter-fiber failures and delaminations. Right: Region above electrodes 1 and 4 (outer electrodes), only inter-fiber failures

Excerpt from ISBN 978-3-00-053387-7

The comparison of the regions close to the outer electrodes and close to the inner electrodes shows that the only difference is the presence of delaminations in the higher loaded (center) area. Inter-fiber failures in the 90°-layers are present in all areas. Since the resistance change increases only for measurements with electrodes close to the most loaded areas where delaminations occur, delaminations can be detected by a significantly higher resistance change compared to areas where only inter-fiber failures occur, which are not detected by the through-thickness measurements.

## 5. Conclusion

Ink-jet printed silver nanoparticle ink on CFRP allows for *in situ* monitoring and detection of both, surface cracks and certain defects inside of the CFRP. If inter-fiber failures occur on the surface, the electrical resistance measured along single printed paths increases due to interruptions of the printed paths, which have a lower resistance than the CFRP. Failures inside of the material can be detected by measuring the electrical resistance through the CFRP. With the through thickness measurements delaminations can be detected by an increase of the electrical resistance. If multiple electrodes are printed on the material surface and several measurements are conducted synchronously, a localization of the defects is possible. Hence, in case of intelligent designs of printed paths a detection and a localization of inter-fiber failures and delaminations in CFRP is possible.

## Acknowledgements

We gratefully acknowledge the financial support from Landesforschungsförderung Hamburg.

## References

- [1] Diamanti K, Soutis C. Structural health monitoring techniques for aircraft composite structures. *Progress in Aerospace Sciences* 2010;46(8):342–52.
- [2] Majumder M, Gangopadhyay TK, Chakraborty AK, Dasgupta K, Bhattacharya DK. Fibre Bragg gratings in structural health monitoring—Present status and applications. *Sensors and Actuators A: Physical* 2008;147(1):150–64.
- [3] Kessler SS, Spearing SM, Soutis C. Damage detection in composite materials using Lamb wave methods. *Smart Mater. Struct.* 2002;11(2):269–78.
- [4] Cai J, Qiu L, Yuan S, Shi L, Liu P, Liang D. Structural Health Monitoring for Composite Materials. In: Zulkhair Mansurov, Aida Kistaubaeva, Azhar Zhubanova, Ilya Digel, Irina Savitskaya, Makhmut Biisenbaev et al., editors. *Heterogeneous Composites on the Basis of Microbial Cells and Nanostructured Carbonized Sorbents*: INTECH Open Access Publisher; 2012.
- [5] Staszewski WJ, Boller C, Tomlinson GR. *Health Monitoring of Aerospace Structures*. Chichester, UK: John Wiley & Sons, Ltd; 2003.
- [6] Kang I, Schulz MJ, Kim JH, Shanov V, Shi D. A carbon nanotube strain sensor for structural health monitoring. *Smart Mater. Struct.* 2006;15(3):737–48.
- [7] Chung DDL. Structural health monitoring by electrical resistance measurement. *Smart Mater. Struct.* 2001;10(4):624–36.
- [8] Schulte K, Baron C. Load and failure analyses of CFRP laminates by means of electrical resistivity measurements. *Composites Science and Technology* 1989;36(1):63–76.
- [9] Abry J. In situ detection of damage in CFRP laminates by electrical resistance measurements. *Composites Science and Technology* 1999;59(6):925–35.
- [10] Wen J, Xia Z, Choy F. Damage detection of carbon fiber reinforced polymer composites via electrical resistance measurement. *Composites Part B: Engineering* 2011;42(1):77–86.

- [11] Kaddour A, Al-Salehi F, Al-Hassani S, Hinton M. Electrical resistance measurement technique for detecting failure in CFRP materials at high strain rates. *Composites Science and Technology* 1994;51(3):377–85.
- [12] Schueler R, Joshi SP, Schulte K. Damage detection in CFRP by electrical conductivity mapping. *Composites Science and Technology* 2001;61(6):921–30.
- [13] Kupke M, Schulte K, Schüler R. Non-destructive testing of FRP by d.c. and a.c. electrical methods. *Composites Science and Technology* 2001;61(6):837–47.
- [14] Lee H, Chou K, Huang K. Inkjet printing of nanosized silver colloids. *Nanotechnology* 2005;16(10):2436.
- [15] Smith PJ, Shin D, Stringer JE, Derby B, Reis N. Direct ink-jet printing and low temperature conversion of conductive silver patterns. *J Mater Sci* 2006;41(13):4153–8.
- [16] Perelaer J, Hendriks CE, de Laat, Antonius W M, Schubert US. One-step inkjet printing of conductive silver tracks on polymer substrates. *Nanotechnology* 2009;20(16):165303.
- [17] Kim HS, Kang JS, Park JS, Hahn HT, Jung HC, Joung JW. Inkjet printed electronics for multifunctional composite structure. *Composites Science and Technology* 2009;69(7-8):1256–64.